

Simultaneous registration of structural and diffusion weighed images using the full DTI information.

Hélène Nadeau^{*a}, Yaqiong Chai^b, Paul Thompson^c and Natasha Lepore^{b,c}

^aDawson College, Montreal, Canada. ^bChildren's Hospital of Los Angeles, USA. ^cUniversity of Southern California, USA.

ABSTRACT

Banks of high-quality, multimodal neurological images offer new possibilities for analyses based on brain registration. To take full advantage of these, current algorithms should be significantly enhanced. We present here a new brain registration method driven simultaneously by the structural intensity and the total diffusion information of MRI scans. Using the two modalities together allows for a better alignment of general and specific aspects of the anatomy. Furthermore, keeping the full diffusion tensor in the cost function, rather than only some of its scalar measures, will allow for a thorough statistical analysis once the Jacobian of the transformation is obtained.

Keywords: bimodal registration, MRI, diffusion tensor imaging.

1 INTRODUCTION

Detailed images of the brain can now be obtained from various noninvasive imaging techniques. These techniques are often complementary and combining them allow for more thorough investigations. In particular, it is becoming more common to perform a structural magnetic resonance T1-weighted scan immediately followed by a diffusion weighed scan on a given subject. The two types of images can then be processed and analysed together to get a detailed picture of the brain and to compare it to other brains through a registration.

In recent years, registering anatomical and diffusion magnetic resonance imaging to study white matter structures in the brain has shown a great deal of potential^{1,2,3} but also great challenges. On the one hand, the purely structural registration works well where there are clear contrasts and therefore is efficient at aligning borders. On the other hand, the diffusion data is more sensitive to details of structure and more appropriate to align fibers.

At first sight, it would seem that one could take a method that proved efficient at registering the T1 images and extend it to include the diffusion tensors. In practice, this is far from being simple. First of all, the diffusion data is noisy, which tends to introduce instabilities in the registration. In general, it requires more fine-tuning than its structural counterpart. In addition, DTI tensors are defined in a non-Euclidean space which means that we cannot differentiate or interpolate them using Euclidean operations. This problem can be resolved by working with the logarithm of the tensors, which obey Euclidean relations⁴. Another closely related issue is that tensors need to be reoriented to follow realignment of structures⁵.

Several algorithms focussing on fibers have been proposed. Silless et al.¹ have added geometric constraints to a diffeomorphic Demons registration algorithm in order to improve fiber alignment. In this approach, the algorithm is

* hnadeau@place.dawsoncollege.qc.ca

designed to align some specific fibers as well as the T1 images. In Durrleman et al.⁶ fiber bundles are compared using a metric on currents. Other methods do not embed the fibers in the cost function but apply a similarity measure directly on the diffusion tensors^{7,8}. Chiang et al.⁹ have used information theory and Kullback-Leibler divergence between probability density functions for cost metric. Malinsky et al.² have registered the fractional anisotropy together with the T1 images. Finally, the two-dimensional tensors may not even capture enough of the complexity of the fibers and it has been proposed by Barpoutis et al.¹⁰ to register fourth-order tensors as well.

Here we present a method that aligns simultaneously the whole diffusion tensors and the T1 images, with the goal to perform statistics on all aspects of diffusion and structure once the registration is done. To do so, we use a fluid regularizer on Navier-Stokes equation as in¹¹ and impose forward-backward symmetry^{12,9}. In order to have flexibility, we weigh locally the relative strengths of the T1 and DTI contributions to the force driving the registration. Scalar measures such as the fractional anisotropy or the mean diffusivity are used as criteria to set the relative weights. To our knowledge, this is the first time that this cost function and all of these algorithms are combined together.

In this preliminary study, our method is tested by registering unto each other two brains of healthy patients from the Alzheimer's Disease Neuroimaging Initiative ADNI-2 database.

2 METHOD

We assume the deforming brain to act as a fluid, so as to allow for smooth and possibly large deformations. Following Christensen et al.¹¹, we apply a non-linear registration based on the Navier-Poisson fluid-dynamical equations where:

$$\mathbf{F} + \mu \nabla^2 \mathbf{v}(x, t) + (\lambda + \mu) \nabla \nabla^T \mathbf{v}(x, t) = 0 \quad , \quad (1)$$

where \mathbf{F} is the force driving the registration, \mathbf{v} is the velocity field and μ and λ are the equivalent of viscosity coefficients, set to keep a smooth transformation, and x is a three-dimensional vector. Our code is a direct extension of the one that was used in Lepore et al.¹³ and the main steps of our registration follow the ones described in Brun et al.¹⁴. The registration is not very sensitive to variations of μ and λ , so we set them both equal to 1. We use a Bro-Nielsen-Gramkow filter¹⁵ to speed up the solution of the differential equation for the velocity with a five-point gaussian.

Our cost function is composed of the square of the intensity difference for the structural part and the square of the log-Euclidean differences for the diffusion part. Since the diffusion tensors fall on a conical manifold of positive-definite matrices, the log is used to project their values to the tangent plane at the origin to enable Euclidian computations⁶:

$$E = \alpha \int_{\Omega} \left\{ [I_T(x - u(x)) - I_S(x)]^2 \right\} dx^3 + \beta \int_{\Omega} \text{Tr} \left\{ [\log D_T(x - u(x)) - \log D_S(x)]^2 \right\} dx^3 \quad . \quad (2)$$

The functions I_T and I_S are the intensities of the target and subject *T1* scans respectively, D_T and D_S are the diffusions tensors for the same target and subject, and u is the displacement. The parameters α and β are relative weights that are adjusted locally, allowing the registration to be driven more heavily by the diffusion tensors in white matter and more heavily by the structural information elsewhere. Typically, we set $\beta=5$ and $\alpha=0$ in regions where the fractional anisotropy is larger than 0.5, and $\beta=0$ and $\alpha=1$ elsewhere, but other schemes are possible as well.

Minimization of the cost function (2) with respect of variation of the vectorial displacement field $u(x)$ gives the following driving force:

$$\mathbf{F}(x, u(x, t)) = \alpha \mathbf{F}_{\text{structure}}(x, u(x, t)) + \beta \mathbf{F}_{\text{diffusion}}(x, u(x, t)) \quad , \quad (3)$$

with:

$$\mathbf{F}_{\text{structure}}(x, u(x, t)) = -[I_T(x - u(x, t)) - I_S(x)] \nabla I_T|_{x=u(x, t)} \quad , \quad (4)$$

$$F_{\text{diffusion}}(x, u(x, t)) = -\text{Tr}\{[\log D_T(x - u(x)) - \log D_S(x)] \nabla \log D_T|_{x=u(x, t)}\} . \quad (5)$$

The forces are normalized so that the structural and diffusion components are of the same order of magnitude. The normalisation factor for $F_{\text{structure}}$ is simply the maximum value it takes on the grid, and the same number is used for all three directions. For $F_{\text{diffusion}}$, we consider any value further than two standard deviations from the mean to be an outlier, produced by noise or unstable data. We bring back these outliers to the closest limit of the range:

$$\text{If } F_{\text{diffusion}}(x, y, z) > \langle F_{\text{diffusion}}(x, y, z) \rangle + 2\sigma \text{ then } F_{\text{diffusion}}(x, y, z) = \langle F_{\text{diffusion}}(x, y, z) \rangle + 2\sigma , \quad (6a)$$

$$\text{If } F_{\text{diffusion}}(x, y, z) < \langle F_{\text{diffusion}}(x, y, z) \rangle - 2\sigma \text{ then } F_{\text{diffusion}}(x, y, z) = \langle F_{\text{diffusion}}(x, y, z) \rangle - 2\sigma . \quad (6b)$$

Then we normalize by dividing every value in the grid in all directions by $\langle F_{\text{diffusion}} \rangle + 2\sigma$.

We enforce forward-backward symmetry using the method of Leow et al.¹² and Chiang et al.⁹. As the anatomical structures are warped, the directions of the diffusion tensors should be reoriented accordingly. For this, we apply the method of Alexander et al.⁵, at each voxel and at each time step. To keep a good balance between effectiveness and quality of registration, we have adopted a multi-resolution scheme¹⁶ with variable time steps and number of iterations. As we warp an image into another, we need to estimate the values of the fields in locations intermediate to the centers of the voxels of the original image. A linear interpolation works well for the structural intensities, but a nearest-neighbour assignment gives better results for the diffusion tensors.

We apply our method here to the registration of two whole brains from healthy senior subjects from the Alzheimer's Disease Neuroimaging Initiative ADNI-2 database. The T1 and DW images were acquired from a 3T GE scanner with 41 gradient directions. The DW images were aligned to the first b0 scan and Eddy current corrected using FSL4.1 in a preprocessing done by the database management. We mask and spatially normalize the T1 images and estimate the tensors using FSL, then co-register and correct the diffusion images using 3DMI from LONI. Finally, the tensors were reconstructed in our program from the eigenvectors and eigenvalues provided by preprocessing.

3 RESULTS AND DISCUSSION

Our method gives good results for the registration as can be seen in Figures 1 and 2. Though our program has the capability to register at three different resolutions consecutively, we get better results when we do around 20 iterations only at the resolution of the voxel size. While ensuring forward-backward symmetry^{9,12}, we register simultaneously the target image on the subject image and vice-versa.

The results presented here all come from a 3D registration over the whole brain. To illustrate the alignment of the principal fibers, we reproduce only the axial slices at mid-height, but the discussion is valid for other white-matter structures as well.

Figure 1 shows an axial slice at mid-height of the original and registered T1 images of two brains. The general shape and the main white-matter structures are well registered. The cortical regions are less so, as is typical in whole brain registrations. We have recently extended the algorithms here to a combined cortical-whole brain fluid registration that improved cortical matching¹⁷. While we focus on the simpler whole brain fluid registration in this paper, the next step will be to extend the method to using this combined algorithm in conjunction with the diffusion information. As a measure of the quality of the registration of the diffusion data, we consider the fractional anisotropy in Figure 2, for the slices and subjects of Figure 1. The main fibers are well-registered, but very narrow structures are sensitive to noise.

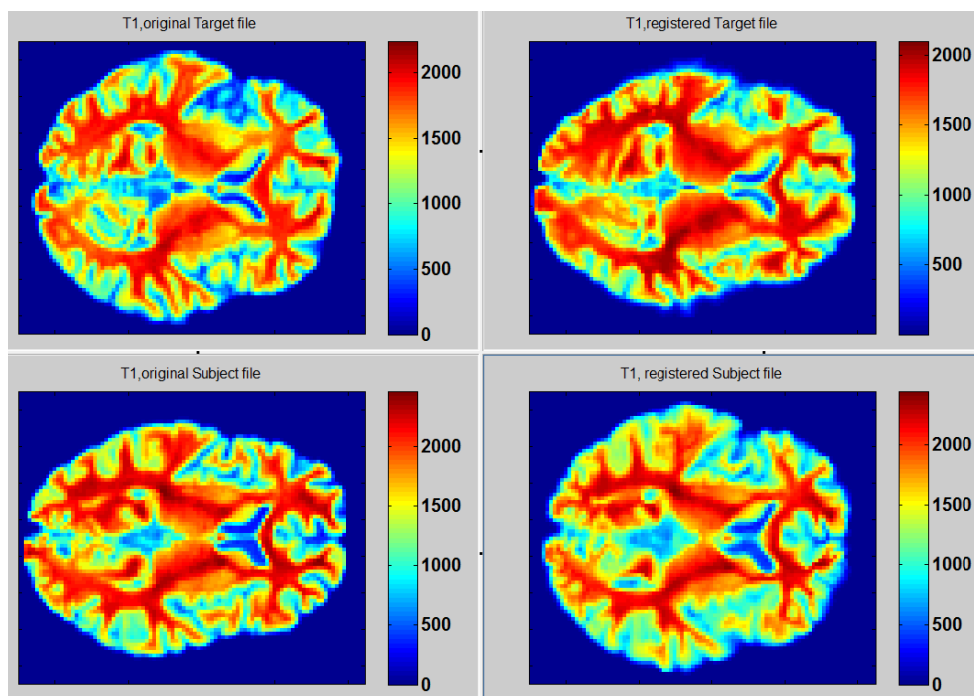


Figure 1: Axial slices at mid-height of T1 images. The target is in the top row, the subject in the bottom row, the original figures in the left column and the registered ones in the right column. Comparing figures on the diagonal shows a very good registration of the general shape and the main white-matter structures.

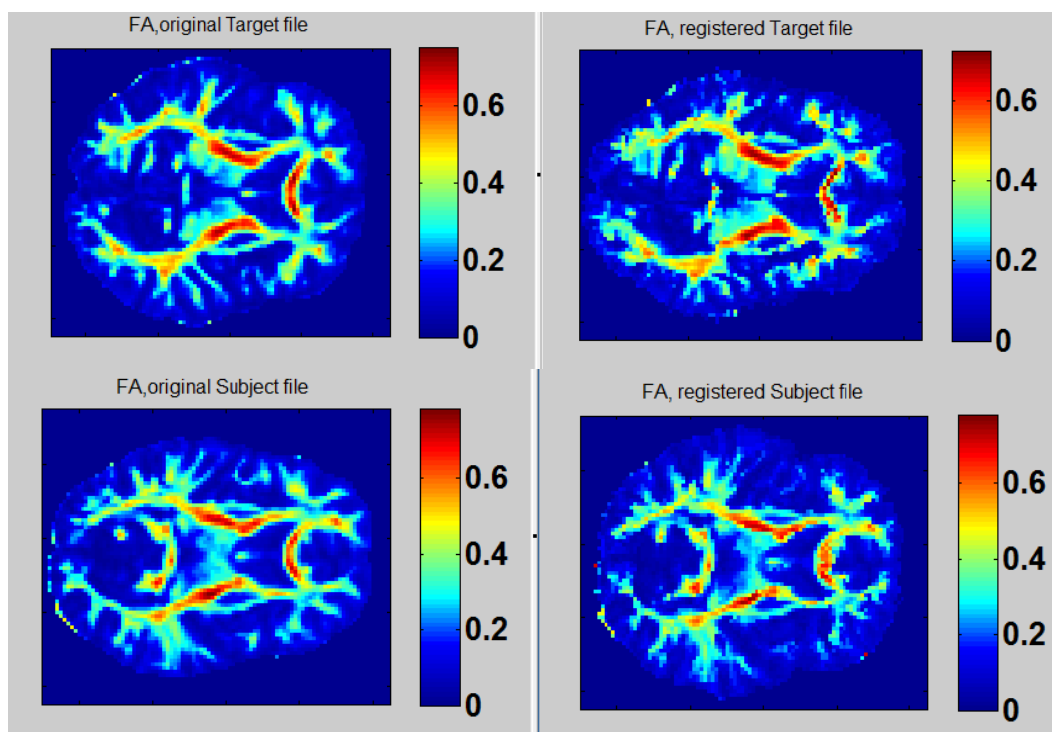


Figure 2 Axial slices at mid-height of FA of original and registered diffusion tensors. The target is in the top row, the subject in the bottom row, the original figures in the left column and the registered ones in the right column. Comparing figures on the diagonal shows a good registration of the main fibers.

We manually set α and β , the relative weights of the T1 and DTI contributions to the registration. We have tried various combinations and observed that the main fibers are reasonably well-aligned when, $\beta=5$ and $\alpha=0$ in regions where the fractional anisotropy is larger than 0.5, and $\beta=0$ and $\alpha=1$. We can see the effect of the parameters α and β by looking at the difference between the registered and the goal image for different combinations of parameters. Figure 3 displays three combinations: 1) $\alpha=1$ and $\beta=0$ where $FA < 0.5$ and $\alpha=0$ and $\beta=5$ everywhere else; 2) $\alpha=1$ and $\beta=0$ where $FA < 0.3$ and $\alpha=0$ and $\beta=5$ everywhere else; 3) $\alpha=1$ and $\beta=0$ everywhere (registration totally driven by the T1 image). The improvement that we see for the sections marked with an arrow indicates that these fibers will align better if the registration is driven by the diffusion tensors only where there is a strongly preferred direction of diffusion.

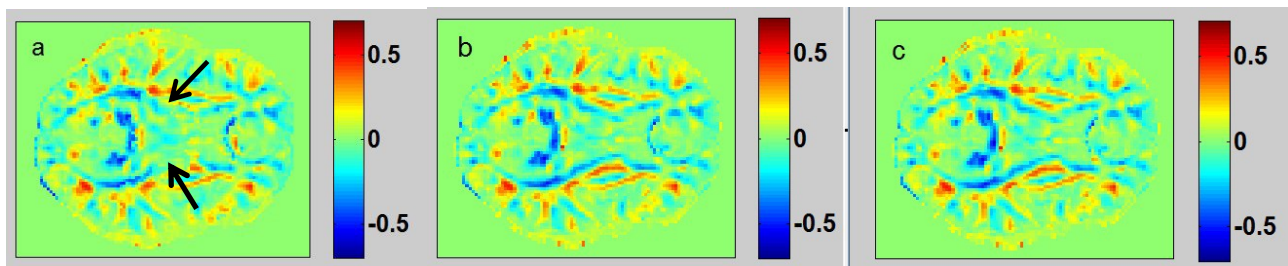


Figure 3 Axial slices at mid-height of (FA of registered image – FA of goal image) for a) $\alpha=1$ and $\beta=0$ where $FA < 0.5$ and $\alpha=0$ and $\beta=5$ everywhere else; b) $\alpha=1$ and $\beta=0$ where $FA < 0.3$ and $\alpha=0$ and $\beta=5$ everywhere else; c) $\alpha=1$ and $\beta=0$ everywhere (registration totally driven by the T1 image).

We are currently working on adding similar constraints using other scalar measures of the diffusion tensors, such as the mean diffusivity, to improve the registration in other parts of the brain. We should stress though that the role of these constraints is only to determine the relative weight of the two components of the force in equation (3) and that the DTI part of the cost function and the related driving force always use the full tensor.

So far, we have focussed on principal fibers but we plan on addressing the problematic of fiber crossing^{18,19}. The second order tensors do not differentiate between a region where two fibers cross and one where the diffusivity is essentially isotropic. To disentangle these we plan on introducing higher order tensors in our model as for example in Barmpoutis et al¹⁰.

4 CONCLUSIONS

We have succeeded in registering simultaneously the T1 and diffusion tensors of two whole brains from healthy subjects from the ADNI data base. This required fine-tuning of the relative weights of the T1 and DTI contributions to the driving force. The method has a lot of potential and it is worth continuing to test it with constraints not only on the fractional anisotropy but other scalar measures as well. We will apply our method on group studies and calculate statistics on the Jacobian of the transformation in a following paper.

This work has not been submitted for publication or presentation elsewhere.

5 ACKNOWLEDGEMENTS

This work was funded through NIH National Institute of Biomedical Imaging and Bioengineering grant R21EB012177. The work of H.N. was supported by a research grant from the Fonds de recherche du Québec, Nature et technologies.

6 REFERENCES

- [1] Siless, V., Glaunès, J., Guevara, P., Mangin, J.-F., Poupon, C., Le Bihan, D., Thirion, B. and Fillard, P., “Joint T1 and Brain Fiber Log-demons Registration using Currents to model Geometry”, MICCAI (2012).
- [2] Malinsky, M., Peter, R., Hodneland, E., Lundervold, A. J., Lundervold, A. and Jan, J., “Registration of FA and T1-Weighted MRI Data of Healthy Human Brain Based on Template Matching and Normalized Cross-Correlation” *Journal of Digital Imaging* , 26 (4), 774-785 (2013).
- [3] Avants, B. B., Duda, J. T., Zhang, H. and Gee, J. C., “Multivariate Normalization with Symmetric Diffeomorphisms for Multivariate Studies”, *Med Image Comput. Comput. Assist Interv.* 10, 359-366 (2007).
- [4] Arsigny, V., Fillard, P., Pennec, X., and Ayache, N. “Log-Euclidean Metrics for fast and simple calculus on diffusion tensors”, *Magnetic Resonance in Medicine*, MRM, 56 (2), 411-421 (2006).
- [5] Alexander, D.C., Pierpaoli, C., Basser, P. J. and Gee, J. C., “Spatial transformations of diffusion tensor magnetic resonance images”, *IEEE Trans. Med. Imaging* 20, 1131–1139 (2001).
- [6] Durrleman, S., Fillard, P., Pennec, X., Trounev, A., Ayache, N., “Registration, atlas estimation and variability analysis of white matter fiber bundles modeled as currents”, *NeuroImage* 55, 1073–1090 (2011).
- [7] Yeo, B.T.T., Vercauteren, T. ; Fillard, P. ; Peyrat, J. ; Pennec, X. ; Golland, P. ; Ayache, N. ; Clatz, O. “Dt-refind: Diffusion tensor registration with exact finite-strain differential”, *IEEE Trans. Med. Imaging* 28, 1914–1928 (2009).
- [8] Zhang, H., Yushkevich, P. A., Alexander, D. C. and Gee, J. C., “Deformable registration of diffusion tensor MR images with explicit orientation optimization”, *Med Image Anal* 10, 764–785 (2006).
- [9] Chiang, M. C., Leow, A.D., Klunder, A. D., Dutton, R. A., Barysheva, M., Rose, S. E., McMahon, K.L., Zubizaray, G. I., Toga, A. W. and Thompson, P. M., “Fluid registration of diffusion tensor images using information theory”, *IEEE Trans. Med. Imaging*, 27, 442-456 (2008).
- [10] Barmptoutis, A., Vemuri, B.C., and Forder, J.R., “Registration of High Angular Resolution Diffusion MRI Images Using 4th Order Tensors”, *Med. Image Comput Comput Assist Interv.* 10, 908-915 (2007).
- [11] Christensen, G. E., Johnson, H. J., “Consistent image registration” *IEEE Transactions on Image Processing*, 20, 568-582 (2001).
- [12] Leow, A., Huang, S.C., Geng, A., Becker, J., Davis, S., Toga, A. and Thompson, P., “Inverse Consistent Mapping in 3D Deformable Image Registration: Its Construction and Statistical Properties”, *Information Processing in Medical Imaging*, *Lecture Notes in Computer Science*, 3565, 493-503 (2005).
- [13] Leporé, N., Chou, Y., Lopez, O.L., Aizentein, H.J., Becker, J.T., Toga, A.W., and Thompson, P.M., “Fast 3D Fluid Registration of Brain Magnetic Resonance Images”, *Proc. SPIE* 6916, *Medical Imaging 2008: Physiology, Function, and Structure from Medical Images*, 69160Z (March 12, 2008);doi:10.1117/12.774338.
- [14] Brun, C., Leporé, N., Pennec, X., Chou, Y., Lopez, O.L., Aizentein, H.J., Becker, J.T., Toga, A.W., and Thompson, P.M., “Comparison of Standard and Riemannian Fluid Registration for Tensor-Based Morphometry in HIV/AIDS”, *Proceedings, MICCAI 2007 Workshop on Statistical Registration: Pair-wise and Group-wise Alignment and Atlas Formation*, Brisbane, Australia, Nov 2 (2007).
- [15] Bro-Nielsen, M., Gramkow, C., “Fast fluid registration of medical images”, *Proceedings of the 4th International Conference on Visualization in Biomedical Computing*, Hamburg, Germany, September 22-25, 267-276 (1996).

- [16] Gramkow, C., “Registration of 2D and 3D medical images”, Master’s thesis, Danish Technical University, Copenhagen, Denmark (1996).
- [17] Lepore, N., Joshi, A.A., Villalon-Reina, J., Brun, c., and Thompson, P.M., “Comparison of 3D image registration algorithms with and without surface constraints for population studies”, SIPAIM-2012 (2012).
- [18] Wiegell, M.R., Larsson, H.B.W., and Wedeen, V.J., “Fiber Crossing in Human Brain Depicted with Diffusion Tensor MR Imaging”, *Radiology*, 27, 897-903 (2000).
- [19] Lenglet, C., Campbell, J.S.W. , Descoteaux, M., Haro, G. ,Savadjiev, P. ,Wassermann, D. ,Anwander, A. , Deriche, R.,Pike, G.B. ,Sapiro, G. ,Siddiqi, K. ,Thompson, P.M. , “Mathematical methods for diffusion MRI processing”, *NeuroImage*, 45, S111–S122 (2009).